













# NanoSSIEFARL polymeric nanoparticles-based immunotherapeutic for the treatment of genital herpes

Renata Zorzetto<sup>1\*</sup> , Flávia Pires Peña<sup>2</sup> , Aline Cláudio de Oliveira<sup>1</sup> ,  
Jayme de Castilhos Ferreira Neto<sup>1</sup> , Gabriel Tardin Mota Hilario<sup>1</sup> ,  
Fernanda Teresa Bovi Frozza<sup>3</sup> , Marvin Paulo Lins<sup>3</sup> , Fernanda Poletto<sup>4</sup> ,  
Marcelo Jung Eberhardt<sup>4</sup> , Pedro Roosevelt Torres Romão<sup>5</sup> , Tanira Alessandra Silveira Aguirre<sup>2</sup> ,  
and Luiz Carlos Rodrigues Junior<sup>1</sup> 

<sup>1</sup>Laboratório de Imunovirologia, Universidade Federal de Ciências da Saúde de Porto Alegre – UFCSPA, Porto Alegre, RS, Brasil

<sup>2</sup>Laboratório de Farmacociências, Universidade Federal de Ciências da Saúde de Porto Alegre – UFCSPA, Porto Alegre, RS, Brasil

<sup>3</sup>Laboratório de Imunoterapia, Universidade Federal de Ciências da Saúde de Porto Alegre – UFCSPA, Porto Alegre, RS, Brasil

<sup>4</sup>Programa de Pós-graduação em Química, Instituto de Química, Universidade Federal do Rio Grande do Sul – UFRGS, Porto Alegre, RS, Brasil

<sup>5</sup>Laboratório de Imunologia Celular, Universidade Federal de Ciências da Saúde de Porto Alegre – UFCSPA, Porto Alegre, RS, Brasil

\*renata.zorzetto90@gmail.com

## Abstract

This study aimed to investigate the therapeutic potential of a nanoparticle formulation containing the immunodominant peptide SSIEFARL from Herpes simplex virus 2 glycoprotein B A against genital herpes. A nanoparticle formulation (NanoSSIEFARL) was engineered and characterized for its physicochemical and immunomodulatory properties. NanoSSIEFARL displayed mean particle size of  $212 \pm 5$  nm, polydispersity index of  $0.12 \pm 0.01$  and zeta potential of  $-7.4 \pm 2.5$  mV, exhibiting spherical morphology. pH stability remained consistent over 30 days (day 0:  $4.5 \pm 0.5$ ; day 30:  $5.0 \pm 0.5$ ). A novel high-performance liquid chromatography method was validated for SSIEFARL quantification. Peptide association efficiency reached  $98.3\% \pm 2.1$ , with  $41.6\% \pm 4.4$  peptide release from nanoparticles after 4 hours. Cytotoxicity assessment revealed cellular viability exceeding 90%, with macrophage uptake observed after 4 hours. Altogether, these results suggest that NanoSSIEFARL is a promising candidate for effective immunotherapy against genital herpes.

**Keywords:** *babassu oil, genital herpes, HPLC, polymeric nanoparticle.*

**How to cite:** Zorzetto, R., Peña, F. P., Oliveira, A. C., Ferreira Neto, J. C., Hilario, G. T. M., Frozza, F. T. B., Lins, M. P., Poletto, F., Eberhardt, M. J., Romão, P. R. T., Aguirre, T. A. S., & Rodrigues Junior, L. C. (2025). NanoSSIEFARL polymeric nanoparticles-based immunotherapeutic for the treatment of genital herpes. *Polímeros: Ciência e Tecnologia*, 35(2), e20250014. <https://doi.org/10.1590/0104-1428.20240042>.

## 1. Introduction

Herpes simplex virus types 1 and 2 (HSV-1, HSV-2) cause oral and genital herpes, respectively<sup>[1,2]</sup>, yet both types can infect both regions. According to the World Health Organization (WHO), it is estimated that 3.7 billion people under the age of 50 are infected with HSV-1 (67%), and 491 million between the ages of 15 and 49 are infected with HSV-2 (13%)<sup>[3]</sup>. HSVs can establish a latent infection in neural ganglia and, upon reactivation, can cause recurrent episodes of oral and/or genital ulcers called cold sores. According to WHO, recurrence of genital herpes affects millions worldwide, causing ongoing discomfort and emotional distress while posing significant challenges for both individuals and public health systems. Latency is controlled

by CD4+ helper T lymphocytes and CD8+ cytotoxic T lymphocytes that keep juxtaposed to the nerve sheath<sup>[4-6]</sup>. In mice, most of these HSV-specific CD8+ T lymphocytes are against the immunodominant peptide SSIEFARL in the viral glycoprotein B<sup>[7]</sup>. The immunodominant peptide SSIEFARL shows great potential for herpes treatment, as demonstrated by its influence on the repertoire of virus-specific CD8+ T cells<sup>[7,8]</sup>. Studies reveal that the presence of this immunodominant epitope not only shapes the CD8+ T cell repertoire in murine models but also affects the hierarchy and functionality of subdominant cells, enhancing the efficacy of the immune response against the virus. Additionally, the priming dynamics of virus-specific CD8+ T cells and

latent retention in ganglia are modulated by this epitope, suggesting that manipulating the immune response around SSIEFARL could provide a promising strategy for controlling and potentially eradicating herpes simplex infection<sup>[8,9]</sup>. Therefore, SSIEFARL could be a promising candidate for vaccines or immunotherapy against HSVs<sup>[9,10]</sup>, since there are no approved vaccines, and the treatment against HSVs includes antiviral drugs such as Aciclovir™, which has been widely associated with drug resistance<sup>[11-13]</sup>.

Although SSIEFARL is a potent peptide for the induction of specific CD8+ T response<sup>[14]</sup> and protection in a herpes murine model<sup>[15]</sup>, it is a small biomolecule, and it cannot be applied freely to the genital mucosa due to possible degradation. Thus, developing a nanoparticle containing SSIEFARL may be crucial for a safe and efficient release of the peptide into the mucosa for studies of immunogenicity/vaccination-challenge and evaluation of protection.

Polymeric nanoparticles are colloidal systems that include nanospheres and nanocapsules, depending on their structure and organization. Nanocapsules are composed of an oily core surrounded by a polymeric envelope, in which drugs or molecules can be dissolved inside the core or entrapped in the polymeric membrane<sup>[16,17]</sup>. Poly( $\epsilon$ -caprolactone) (PCL) is a biodegradable polymer hydrolyzed in physiological conditions in the human body and has called the attention of drug delivery since it can modulate degradation kinetics and release profiles<sup>[18]</sup>. Besides the polymer, the core of some nanoparticles are formed by lipophilic substances chosen following criteria such as drug solubility, absence of toxicity, low risk of polymer degradation, and low oil solubility within the polymer or vice-versa<sup>[19]</sup>. Medium-chain triglycerides (MCT), such as capric/caprylic triglycerides, are commonly used as lipophilic cores of nanocapsules<sup>[20]</sup>.

Nanoparticles with a babassu oil core (BBS) are relatively novel. While BBS-based microemulsions have been tested as a delivery system, our group pioneered the development of polymeric nanoparticles containing poly( $\epsilon$ -caprolactone) and babassu oil for hydrophilic molecule delivery<sup>[21]</sup>. Babassu belongs to the family Arecaceae (Palmae) and genera *Orbignya* and *Attalea*, most commonly found in northern and northeastern Brazil. It is extracted from babassu coconuts, offers various medical benefits and is rich in fatty acids<sup>[22]</sup>. It has been traditionally used for skin care and has shown antitumor and anti-inflammatory properties<sup>[22-24]</sup>, and babassu extraction is a significant income source in Maranhão, promoting sustainable livelihoods<sup>[25]</sup>. A recent study showed that the HLB of BBS is 11.5<sup>[26]</sup>. This high HLB value facilitates interactions with polar molecules. Considering its physicochemical properties, as well as its natural, renewable, and sustainable characteristics, BBS was selected as the core material for nanoparticles designed to incorporate hydrophilic drugs<sup>[21]</sup>, therefore we aim to demonstrate its capability to encapsulate smaller polar biomolecules like the HSV peptide SSIEFARL.

Nanoparticles offer tailored delivery for antigens and immunomodulatory agents in mucosal immunotherapy<sup>[27]</sup>, showing effectiveness in experimental models, suggesting potential for preventive and therapeutic strategies against genital infections<sup>[28]</sup>. For effective local delivery to oral and/or genital mucosa, nanoparticles should ideally be in the 100-500

nm size range, exhibit positive or neutral surface charges to improve adhesion while avoiding excessive irritation, and possess surface characteristics that enhance mucoadhesion and drug release. Even though PCL nanoparticles have a negative surface charge, they have already been widely described for mucosal application<sup>[28]</sup>. Careful optimization of these parameters is essential to maximize the therapeutic efficacy and safety of nanoparticle-based delivery systems. However, to ensure feasibility, the nanocarrier must be non-cytotoxic, have reasonable pharmaceutical loading capability and targeting, and feature controlled release<sup>[29,30]</sup>. This study aims to develop and characterize a nanostructured system containing the peptide SSIEFARL, alongside validating a specific HPLC methodology for peptide quantification. This is the first attempt to describe a polymeric nanoparticle delivery system using babassu oil to encapsulate a peptide for use in murine models genital mucosa and validate a quantification methodology for SSIEFARL using HPLC.

## 2. Materials and Methods

### 2.1 Materials

Babassu oil (*Orbignya oleifera*, Mundo dos Óleos™, Brasília, Brazil), poly( $\epsilon$ -caprolactone) (Sigma-Aldrich™, São Paulo, Brazil), SSIEFARL (MW: 922.03 g/mol) (GenScript™, New Jersey, USA), medium-chain triglycerides (capric and caprylic acids, Delaware™, Porto Alegre, Brazil), polysorbate 80 (Tween™ 80, Sigma-Aldrich, São Paulo, Brazil), acetone (Neon™, Suzano, Brazil), ethanol (Dinâmica™, Indaiatuba, Brazil), acetonitrile (ACN) (Neon™, Suzano, Brazil) and trifluoroacetic acid (TFA) (Sigma-Aldrich™, São Paulo, Brazil). Babassu oil study was registered at SisGen (identification ABCECDB) and its composition was described by Oliveira et al.<sup>[21]</sup> SSIEFARL's degree of purification was 97.43%, and the other reagents used were of analytical grade, while the ACN and TFA were of HPLC grade.

### 2.2 Experimental methods

#### 2.2.1 Development and validation of a high-performance liquid chromatography methodology

The experiments were performed on a Prominence UFLC chromatographic system (Shimadzu™, Barueri, Brazil) consisting of a binary pump (model: LC-20AT), online degasser (model: DGU-20A5), ALS autosampler (model: SIL-20A), column oven (model: CTO-20A), PDA detector (model: SPD-M20A) and communication module (model: CBM-20A). Shimadzu LC-Solution™ software was used for data collection. All spectra were collected for peak identification and peak purity calculations. Analysis was carried out at 214 nm with a Phenomenex Luna™ C18 (2), 3  $\mu$ m, 250 mm  $\times$  4.6 mm, 100 Å column (Torrance, USA), and the column heater temperature was set to 40 °C. The injection volume was 50  $\mu$ L for each sample. Solvent A was formulated with ACN 0.1% (v/v) TFA, and Solvent B was prepared with ultrapure water (Milli-Q™) 0.1% (v/v) TFA. Both phases were degassed by sonication for 20 min. The solvent program was a gradient starting with 21% solvent A for at least 45 min to stabilize the equipment. The gradient program was 0.01-1 min = 21% A and 79%

B; 1-15 min = 45% A and 55% B; 15-17 min = 45% A and 55% B; 17-19 min = 21% A and 79% B; and 19-29 min = 21% A and 79% B. The last 10 min of each run were set for column stabilization before the following sample. The flow rate was set at 0.7 mL min<sup>-1</sup>.

The method was subjected to partial validation to ensure the analytical procedure's capability to quantify SSIEFARL. All stock solutions were freshly prepared by diluting SSIEFARL in ultrapure water at a concentration of 10 µg mL<sup>-1</sup> at the test day. Working solutions were prepared using water as a diluent, unless otherwise stated. For the specificity test, 1 mL of nanoparticles without SSIEFARL (Blank NPs) was transferred to a volumetric flask of 5 mL and completed with the diluent. The sample was filtered using a 0.45 µm syringe filter (FILTRILO™, Colombo, Brazil), and then transferred to a vial. A comparison among chromatograms of Blank NPs and NanoSSIEFARL was performed. For linearity assessment, dilutions were prepared in different concentrations (0.25, 0.50, 1.0, 2.5, and 5.0 µg mL<sup>-1</sup>) from a stock solution. A second linearity test was performed at the same concentrations using the release buffer (acetate buffer pH 4.5) as the diluent.

Intra-day precision (repeatability) was evaluated at a concentration of 1 µg mL<sup>-1</sup> of SSIEFARL from six samples prepared by the same analyst on the same day. Inter-day precision (intermediate precision) was evaluated by comparing six determinations of SSIEFARL in two consecutive days. Precision was given as the relative standard deviation (RSD %). To assess robustness, the peptide SSIEFARL was diluted in ultrapure water at a final concentration of 1 µg mL<sup>-1</sup> and analyzed by HPLC using mobile phases at a deliberated modified acid concentration (0.08% TFA). The detection limit (DL) and the quantitation limit (QL) were calculated using the standard deviation of y-intercepts of regression lines obtained for SSIEFARL in water multiplied by 3.3 and by 10, respectively and divided by the slope estimated from the calibration curve. SSIEFARL solution stability was investigated after a month of storage at -80 ± 1 °C. Every experiment was performed in triplicate.

## 2.2.2 Preparation of the polymeric nanoparticles

The preparation of nanoparticles containing babassu oil was carried out according to Oliveira et al.<sup>[21]</sup> through interfacial polymer deposition. Briefly, to obtain the organic phase, the following reagents were dissolved in 2.5 mL of acetone and 6.75 mL of ethanol at 40 °C: 18 mg of BBS, 50 mg of PCL (14 kDa MW), and 80 µL of MCT. At the last minute of solubilization, 200 µL of an aqueous solution of SSIEFARL at a concentration of 1 mg mL<sup>-1</sup> was injected into the stirring organic phase. The aqueous phase comprised 32.6 mg of polysorbate 80 in 26.2 mL ultrapure water. The procedure for obtaining the nanoparticles was conducted in a water bath at 40 °C by injecting the organic phase into the aqueous phase under magnetic stirring for 10 min. The ethanol and acetone were then evaporated under rotary evaporation, and the final volume was adjusted to 10 mL at a final peptide concentration of 20 µg mL<sup>-1</sup>. This concentration was based on previous tests, which were performed to establish the optimal peptide quantity to be encapsulated. The same protocol was carried out without adding the peptide SSIEFARL to produce the Blank NPs as a control vehicle. Fluorescent-

labeled polymeric nanocapsules (NanoSSIEFARLRh) at a final peptide concentration of 20 µg mL<sup>-1</sup> were prepared in the same way; however, the total amount of PCL was replaced by PCL marked with rhodamine B, which was obtained as described by Poletto et al.<sup>[29]</sup>.

## 2.2.3 Physicochemical characterization of the polymeric nanoparticles

For each batch, the volume-weighted mean diameter (d<sub>4,3</sub>) and the polydispersity index (Span) were assessed using laser diffraction (Mastersizer™ 2000, Malvern, UK). Formulations were diluted using 20 µL of nanoparticles and 10 mL of ultrapure water, and the minimal obscuration index used was 1%. The same dilution was used to verify the z-average (mean diameters), polydispersity index (PDI) by dynamic light scattering using backscatter detection at 173°, and to obtain the zeta potential by electrophoretic mobility using Zetasizer™ nano-ZS ZEN 3600 (Nanoseries™, Malvern, UK), 20 µL of nanoparticles were diluted with 10 mL of NaCl 10 mM. The pH was determined by a potentiometer PH2600 (Instrutherm™, São Paulo, Brazil). To determine the association efficiency (AE %) of the peptide SSIEFARL into the nanoparticles, the ultrafiltration-centrifugation method was carried out using centrifugal filter units of 10 kDa (Millipore™, Cork, Ireland). Three hundred and fifty microliters (350 µL) of the nanoparticles were centrifuged at 3000 rpm for 10 min twice and then at 3500 rpm for another 10 min. The ultrafiltrate was diluted in ultrapure water (1:20) and then transferred into inserts to be analyzed by HPLC. The association efficiency percentage was determined by dividing the difference between the total added peptide concentration (20 µg mL<sup>-1</sup>) and the concentration of free peptide in the ultrafiltrate for the total added peptide concentration and multiplying this result by 100. Regarding stability, both NanoSSIEFARL and Blank NPs were maintained at 2-8 °C for 30 days to compare the pH, association efficiency, particle size, polydispersity index, and zeta potential with day 0. Transmission electron microscopy (TEM) (Tecnai™ G2-12, SpiritBiotwin FEI, 120 kV operating at 80 kV, Jülich, Germany) of NanoSSIEFARL was used to evaluate nanoparticle morphology. The formulations were diluted in ultrapure water (5x), deposited on a 400-mesh Formvar carbon film-coated copper grid, and stained with 2% (w/v) uranyl acetate aqueous solution. Measurements were performed using three different batches for each formulation.

## 2.2.4 Release profile of SSIEFARL from polymeric nanoparticles

The release profile experiments were conducted using acetate buffer pH 4.5 (2.26 g of sodium acetate trihydrate + 1.91 mL acetic acid diluted in 1 L of ultrapure water). Controls were carried out by diluting the peptide SSIEFARL in ultrapure water at a final concentration of 20 µg mL<sup>-1</sup>. For the experiment, each beaker contained 51 mL of buffer and 3 mL of NanoSSIEFARL (n = 4 different batches) or control (n = 5 different dilutions) inside a modified cellulose membrane (average flat width of 25 mm and 14 kDa cut-off, Sigma-Aldrich™, Darmstadt, Germany), which was closed with magnetic closures (Spectra/Por™ Closures, Spectrum Laboratories, Inc., New Jersey, USA). The system was placed under stirring at 37 °C and, at specific time points (0.33, 0.5, 0.75, 1, 2, 4, 6, 8, and 24 h), 1 mL of samples were

collected and filtered using 0.45 µm filters. Free media was replaced at the same volume each time. All the samples were then analyzed by HPLC using the validated methodology.

### 2.2.5 Cell viability assay

Cell viability was assessed by flow cytometry using a viability dye. Briefly, 96-well plates were incubated with  $1 \times 10^5$  J774.A1 macrophages in Dulbecco's Modified Eagle Medium (DMEM, Sigma-Aldrich™, Darmstadt, Germany) low supplemented with 10% fetal bovine serum (FBS, Sigma-Aldrich™, Darmstadt, Germany). The next day, different percentages of SSIEFARL  $20 \mu\text{g mL}^{-1}$ , NanoSSIEFARL  $20 \mu\text{g mL}^{-1}$  and, Blank NPs were added into the wells (15, 30, and 60%) in triplicate for each batch and concentration, as well as 60% of ethanol 70% as death control; negative control was set by cells in culture medium, only. After 24 h of incubation at 37° C, cells were transferred to a cytometry tube, rinsed with 200 µL of phosphate-buffered saline (PBS), centrifuged at 1500 rpm for 5 min, and then marked with 200 µL of viability dye and incubated for 20 min at room temperature, protected from light. After, cells were centrifuged for 5 min at 1500 rpm, washed twice with 200 µL of PBS, and analyzed by flow cytometry on FACSCanto™ II (BD Biosciences, Franklin Lakes, USA).

### 2.2.6 Phagocytosis assay

J774.A1 macrophages were seeded at a density of  $5 \times 10^5$  cells/well in a 24-well plate with 500 µL of DMEM low culture medium containing Penicillin-Streptomycin (Sigma-Aldrich™, Darmstadt, Germany), Amphotericin B (Sigma-Aldrich™, Darmstadt, Germany), and supplemented with 10% FBS. After 24 h, cells were incubated with DMEM without Penicillin-Streptomycin, Amphotericin B, and FBS, in which cells in DMEM (negative control); DMEM with SSIEFARL 60% (v/v); DMEM with Blank NPs 60% (v/v) or DMEM with NanoSSIEFARLrh 60% (v/v) for 4 h at 37 °C. Cell fixation was performed with 300 µL of PBS 1% paraformaldehyde for 10 min at room temperature. Cells were then washed with PBS and incubated with 300 µL of PBS 0.5% Triton™ X-100 (Neon™, Suzano, Brazil) for 20 min at room temperature. After, cells were incubated with Phalloidin Alexa Fluor 488 (Sigma-Aldrich™, Darmstadt, Germany) diluted in PBS 0.5% Triton™ X-100 for 30 min at room temperature. Nuclei staining was performed by adding 200 µL of DAPI (4', 6-diamidino-2'-phenylindole, dihydrochloride) (Sigma-Aldrich™, Darmstadt, Germany) diluted with PBS at a final concentration of  $1 \mu\text{g mL}^{-1}$  for 10 min at room temperature. The samples were washed thoroughly with PBS twice for 5 min to remove all excess dye. The images were analyzed on EVOS FL Auto 2 Imaging Microscope (Invitrogen™, Carlsbad, USA).

### 2.2.7 Statistical analysis

Data were analyzed by GraphPad™ Prism version 9.0.0 (La Jolla, USA), and FlowJo™ Software (BD Biosciences, Franklin Lakes, USA). The results are presented as the mean  $\pm$  standard error of the mean (SEM) or mean  $\pm$  standard deviation (SD). Student's t-test and ANOVA were also performed.

## 3. Results and Discussions

### 3.1 Development and validation of a high-performance liquid chromatography methodology

Our group has already developed a specific HPLC methodology with fluorescent quantification of SSIEFARL (MW: 922.03 g/mol)<sup>[30]</sup>. However, here we have described a novel nanoparticle that is constituted by different raw materials, including a different polymer. Therefore, we developed and partially validated a methodology according to the International Conference on Harmonization of Technical Requirements for Pharmaceuticals for Human Use (ICH)<sup>[31]</sup> and RDC N° 166/ 2017 from ANVISA<sup>[32]</sup> considering the following parameters: selectivity, linearity, precision, robustness, limit of detection, and limit of quantification.

The first step was to select and optimize the chromatographic conditions to quantify SSIEFARL by HPLC-DAD. We initiated with traditional parameters for peptide analysis testing C18 reverse phase columns, different gradient programs using ACN plus TFA and water plus TFA as mobile phases, and wavelengths at which the peptide showed absorption. The final methodology results showed no interference at SSIEFARL's retention time ( $14.0 \pm 0.5$  min) from the other formulation components. Therefore, it was possible to confirm the selectivity of the HPLC methodology. The linearity of our HPLC methodology was performed for three individual curves using water or acetate buffer pH 4.5 as diluent. A linear relationship between peak area and concentration of SSIEFARL was observed between 0.25 and  $5.0 \mu\text{g mL}^{-1}$ . A 2D graph where  $y$  is the peak area and  $x$  is the standard solution concentration at  $\mu\text{g mL}^{-1}$  was plotted for each curve, and the linear equation obtained by the least square method for SSIEFARL in water was  $y = 17792x - 403.69$  and for SSIEFARL in pH 4.5 buffer was  $y = 19379x - 1139.10$ . The coefficient of determination obtained ( $r^2$ ) was 0.9997 and 0.9999, respectively, for water and buffer, which makes it possible to conclude that the proposed method is linear. In general,  $r^2$  values near 1 indicate linearity<sup>[33]</sup>.

Regarding precision, repeatability (intra-day), and intermediate precision (inter-day), the results are shown in Table 1. Accuracy may be inferred, since the method showed precision, linearity, and specificity<sup>[31]</sup>

**Table 1.** Repeatability (intra-day) and intermediate precision (inter-day) of the HPLC method.

Theoretical Concentration	Day	Mean analytical Concentration ( $\mu\text{g mL}^{-1}$ )	RSD (%)
<b>Repeatability (n = 6/day)</b>			
$1 \mu\text{g mL}^{-1}$	1	0.95	5.95
	2	0.97	5.38
<b>Intermediate precision (n = 12)</b>			
$1 \mu\text{g mL}^{-1}$	-	0.96	5.53



The influence of variations in mobile phase composition was used as a parameter to investigate robustness<sup>[34]</sup>. After some tests, the RSD (%) determined for samples at a concentration of  $1 \mu\text{g mL}^{-1}$  on the same day with the correct mobile phase (0.1% TFA) and modified mobile phase (0.08%) was 4.7%. Since the RSD values did not exceed 5%, the proposed HPLC methodology can be considered robust for SSIEFARL<sup>[35]</sup>. The detection limit of the method was calculated as  $0.063 \pm 0.008 \mu\text{g mL}^{-1}$ , and the quantitation limit was calculated as  $0.190 \pm 0.020 \mu\text{g mL}^{-1}$ . Therefore, the range at which the developed HPLC methodology provides an acceptable degree of linearity, accuracy and precision was determined as 0.2 to  $5.0 \mu\text{g mL}^{-1}$ .

### 3.2 Preparation and characterization of polymeric nanoparticles

The nanoparticle formulations were prepared as previously described<sup>[21]</sup>. The average particle size of NanoSSIEFARL and Blank NPs obtained with laser diffraction (Figure 1a) and DLS (Figure 1b), the polydispersity indexes, zeta potential and pH values are discriminated in Table 2. The image obtained with transmission electron microscopy (Figure 1c) showed a spherical nanoparticle with approximately 200 nm for NanoSSIEFARL, similar to nanoparticles without peptide. The evaluated parameters did not show significant changes after 30 days at 2-8 °C, indicating that the nanoparticles have good stability and can be used in *in vitro* experiments.

Nanoparticles produced using the polymer's interfacial deposition method have a mean diameter of 200-300 nm<sup>[36]</sup>, consistent with the size of NanoSSIEFARL. Blank nanoparticles have a mean diameter of 179-190 nm, with no significant statistical difference observed when comparing them to NanoSSIEFARL. Overall, statistical analysis indicates similarities in mean diameters, PDI and Span values, zeta potentials, and pH values between formulations with or without SSIEFARL ( $p > 0.05$ ), therefore concluding that NanoSSIEFARL showed all the characteristics of a polymeric nanoparticle.

Regarding the nanoparticle nucleus, we have previously shown that babassu oil allows the encapsulation of substances with hydrophilic characteristics<sup>[21]</sup>, but these particles were used here for the first time to associate a biomolecule. A novel HPLC methodology was also used to determine the association efficiency of the peptide SSIEFARL to the nanoparticles following centrifugation-ultrafiltration, which showed the % AE of  $98.3 \pm 2.1\%$ . Usually, the lipid core in polymeric nanoparticles plays a crucial role in delivering therapeutic agents, providing a conducive environment for the efficient encapsulation of hydrophobic drugs. Nevertheless, using this same principle, but employing an oil with elevated required HLB, we were able to associate SSIEFARL with polymeric nanoparticles.

Advances in peptide encapsulation show promise, yet challenges remain in optimizing formulations for different peptides and ensuring stability. Nanoparticles protect peptides, enhance absorption, and improve therapeutic efficacy<sup>[37-39]</sup>. Various polymeric nanosystems serve as effective peptide carriers, including chitosan- and dextran-based nanoparticles, PLGA nanocarriers, and PCL-based nanoparticles<sup>[37,40-44]</sup>.

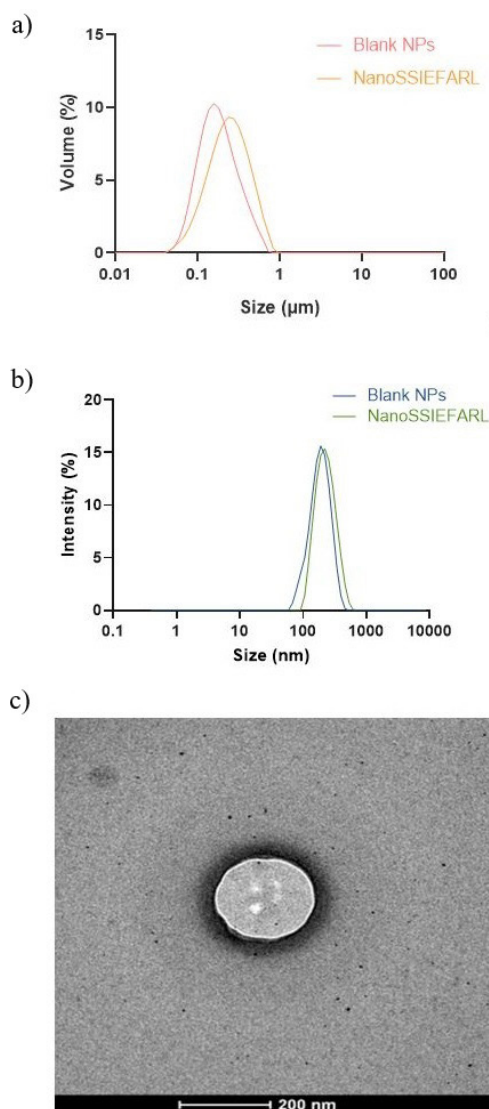


**Figure 1.** (a) Typical particle size distribution of NanoSSIEFARL and Blank NPs obtained with laser diffraction; (b) Typical particle size distribution of NanoSSIEFARL and Blank NPs using the CONTIN algorithm from DLS measurements; (c) Transmission electron microscopy image of a NanoSSIEFARL particle stained with uranyl acetate (magnification = 100.000x, scale bar = 200nm).

### 3.3 SSIEFARL's release profile in the nanoparticle system

The release was carried at pH 4.5 to mimic the infected HSV genital mucosa. The amount of SSIEFARL released from the nanoparticles was  $41.6\% \pm 4.4$  at 4 hours and  $63.0\% \pm 6.9$  at 24 hours of the theoretical amount incorporated ( $20 \mu\text{g mL}^{-1}$ ). In contrast, the control (SSIEFARL in ultrapure water) exhibited a faster release rate, with  $57.6\% \pm 3.3$  released at 4 hours and  $84.7\% \pm 1.8$  at 24 hours (Figure 2). This difference may be attributed to the presence of SSIEFARL still within the nanoparticles or at the interface between the particles and the dispersant medium inside the cellulose bag. As a result, diffusion processes are required to release SSIEFARL into the medium, making the release from the nanoparticles slower compared to the control.

**Table 2.** Mean size (d[4,3]; z-average), polydispersity (Span), polydispersity index (PDI) and zeta potential of Blank NPs and NanoSSIEFARL.

Formulation	d[4,3] (nm)	Span	z-average (nm)	PDI	Zeta Potential (mV)	pH
Blank NPs (T0)	190 ± 48	1.44 ± 0.26	179 ± 37	0.08 ± 0.01	-8.3 ± 2.4	4.9 ± 0.2
Blank NPs (T30)	189 ± 57	1.28 ± 0.37	182 ± 45	0.10 ± 0.01	-8.2 ± 1.3	5.5 ± 0.7
NanoSSIEFARL (T0)	255 ± 15	1.55 ± 0.09	212 ± 5	0.12 ± 0.01	-7.4 ± 2.5	4.5 ± 0.5
NanoSSIEFARL (T30)	252 ± 32	1.59 ± 0.12	211 ± 10	0.10 ± 0.02	-9.2 ± 1.9	5.0 ± 0.5

Results expressed as mean ± standard deviation (n = 3).

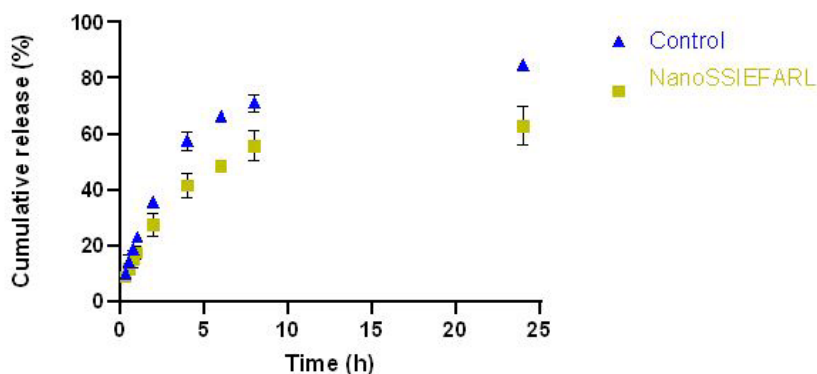


**Figure 2.** Cumulative release percentage of NanoSSIEFARL in comparison to control (SSIEFARL in ultrapure water) throughout time. Data are expressed as mean ± SD (n = 4-5).

Our group was the first to study the association of the immunodominant peptide SSIEFARL, derived from viral glycoprotein B of HSV2, to polymeric nanoparticles<sup>[30]</sup>. However, this earlier system showed only 4.9% SSIEFARL association with the nanoparticle and 25% drug release after 24 h<sup>[30]</sup>. Here, our data showed that the release of the peptide from the nanoparticle formulation (NanoSSIEFARL) was found to be lower in comparison to the control solution, indicating that the nanoparticles effectively function as a protective carrier. This mechanism allows for the intact delivery of the peptide, thereby enhancing its therapeutic efficacy. While the release profile can be characterized as both controlled and prolonged, it is crucial to highlight that the primary role of the nanoparticle system is to safeguard the peptide. The controlled release is driven by the diffusion processes of the peptide through the nanoparticle matrix, while the prolonged release minimizes the risk of a burst effect - a phenomenon often observed with conventional dosage forms, such as tablets, where the drug is released in a single rapid discharge. Additionally, the observed similarity in release profiles between the nanoparticle formulation and the control solution suggests that the peptide undergoes no significant chemical alterations during the release process, thereby ensuring the retention of its therapeutic properties. This dual function of protection and sustained release positions NanoSSIEFARL as a promising candidate for enhancing the delivery and efficacy of therapeutic peptides. Furthermore, this finding is relevant considering that dendritic cells and macrophages are expected to take up nanoparticles, which usually need 3 to 4 h to occur<sup>[45,46]</sup>, and that the peptide antigenic presentation can induce a specific immune response.

### 3.4 NanoSSIEFARL is non-cytotoxic and efficiently phagocytosed by macrophages *in vitro*

Before testing whether macrophages phagocytize NanoSSIEFARL, cytotoxicity was evaluated by flow cytometry. Cells were incubated with alcohol (negative control), medium, and different concentrations of SSIEFARL, Blank NPs, or NanoSSIEFARL, and the viability was evaluated by AmCyan A staining as illustrated in Figure 3a. It was observed that the macrophages viability was not inhibited by the treatments with Blank NPs, SSIEFARL or NanoSSIEFARL (Figure 3b). To evaluate the nanoparticle effect on cells of interest, cytotoxicity must be assessed with cells representing the exposure route<sup>[47]</sup>. Thus, we used J774.A1 macrophages since macrophages are one of the first cells to recognize and uptake nanoparticles after topical application, and because it is an important antigen-presenting cell (APC) for T cell activation<sup>[47]</sup>.

NanoSSIEFARL Rhodamine B (NanoSSIEFARLRh) was used at a final concentration of 12 µg mL<sup>-1</sup> (60% v/v) per well to perform the phagocytosis assay. This formulation was characterized in terms of size and presented no statistical difference to NanoSSIEFARL particles. Figure 3c shows macrophages without any treatment (negative control) or treated with SSIEFARL Rhodamine B (SSIEFARLRh). As can be observed, SSIEFARL itself, marked with Rhodamine B, was not uptaken. Since it is a small peptide, it probably suffered degradation without nanoencapsulation and, therefore, does not show fluorescence. Figure 3d shows macrophages incubated with NanoSSIEFARLRh, and red arrows indicate the phagocytosis of NanoSSIEFARLRh.

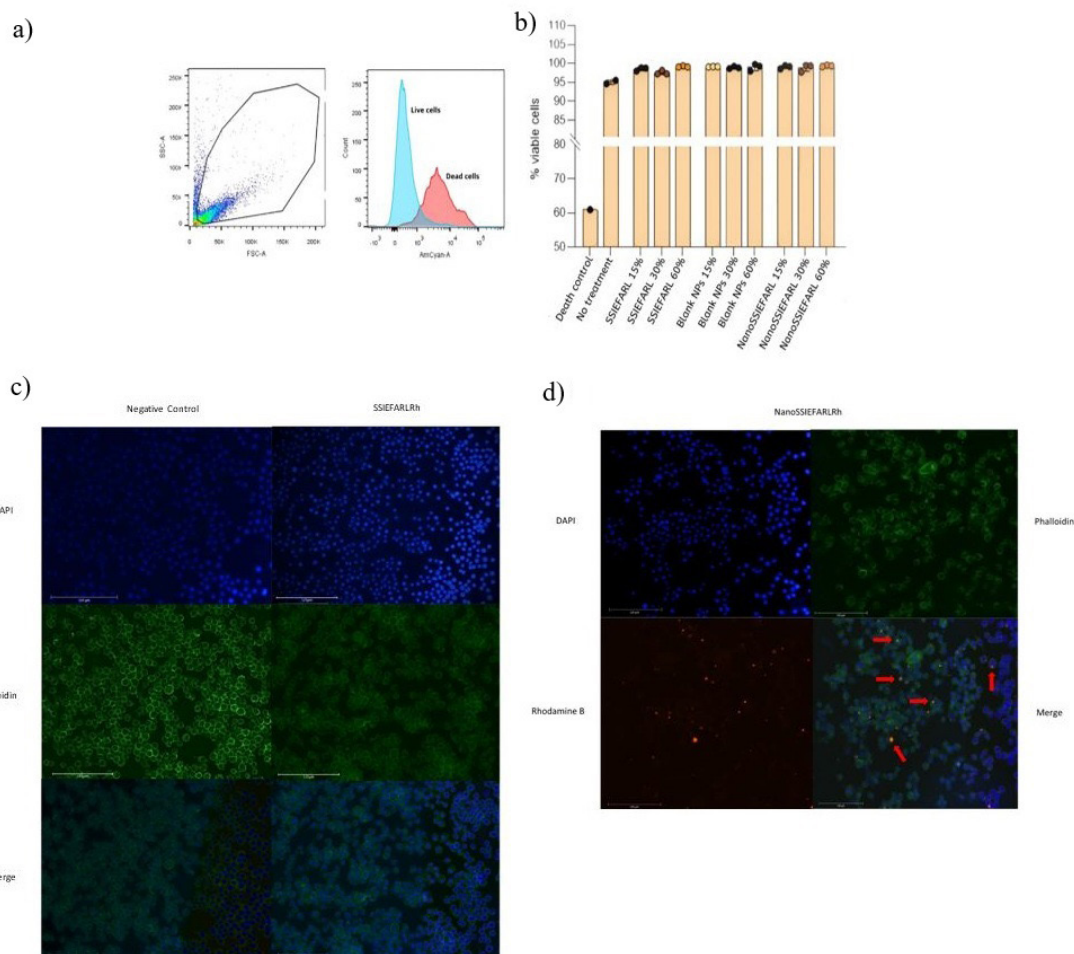


**Figure 3.** Cell viability and phagocytosis of NanoSSIEFARLrh by J774.A1 macrophages: (a) Gating strategy with AmCyan A to characterize live and dead cells; (b) Percentage of viable cells in all groups. Data shown are for mean  $\pm$  SD (n=3); (c) J774.A1 macrophages untreated and treated with SSIEFARLrh; (d) J774.A1 macrophages treated with NanoSSIEFARLrh. Groups were marked with DAPI (blue, nuclei dye), Phalloidin Alexa Fluor 488 (green, cytoskeleton dye), Rhodamine B (red), and MERGE. Red arrows indicate nanoparticle uptake by macrophages. (Magnification 200x).

## 4. Conclusions

Here, we showed the production and characterization of a polymeric nanoparticle containing babassu oil with a high association efficiency of SSIEFARL. NanoSSIEFARL exhibited spherical morphology with a diameter of approximately 200 nm. pH stability was maintained over a month. Nanoparticles presented adequate characteristics in terms of size, homogeneity, and stability, and a specific HPLC methodology to quantify the peptide was developed, showing parameters according to the required legislation. Nanoparticles were safe to J774.A1 macrophages and were phagocytosed by them after 4 hours. In conclusion, NanoSSIEFARL showed promising results, suggesting that it may be a strong candidate for further research into new treatments for genital herpes.

## 5. Author's Contribution

- **Conceptualization** – Renata Zorzetto; Tanira Alessandra Silveira Aguirre; Luiz Carlos Rodrigues Junior.

- **Data curation** – Renata Zorzetto; Tanira Alessandra Silveira Aguirre; Luiz Carlos Rodrigues Junior.
- **Formal analysis** – Renata Zorzetto; Flávia Pires Peña; Gabriel Tardin Mota Hilario; Aline Cláudio de Oliveira; Jayme de Castilhos Ferreira Neto.
- **Funding acquisition** – NA.
- **Investigation** – Renata Zorzetto; Flávia Pires Peña; Gabriel Tardin Mota Hilario; Aline Cláudio de Oliveira; Jayme de Castilhos Ferreira Neto.
- **Methodology** – Renata Zorzetto; Flávia Pires Peña; Gabriel Tardin Mota Hilario; Aline Cláudio de Oliveira; Fernanda Teresa Bovi Frozza; Marvin Paulo Lins; Fernanda Poletto; Marcelo Jung Eberhardt; Tanira Alessandra Silveira Aguirre; Luiz Carlos Rodrigues Junior.
- **Project administration** – Renata Zorzetto; Tanira Alessandra Silveira Aguirre; Luiz Carlos Rodrigues Junior.



- **Resources** – Fernanda Poletto; Pedro Roosevelt Torres Romão; Tanira Alessandra Silveira Aguirre; Luiz Carlos Rodrigues Junior.
- **Software** – NA.
- **Supervision** – Renata Zorzetto; Tanira Alessandra Silveira Aguirre; Luiz Carlos Rodrigues Junior.
- **Validation** – Renata Zorzetto; Flávia Pires Peña; Tanira Alessandra Silveira Aguirre; Luiz Carlos Rodrigues Junior.
- **Visualization** – Renata Zorzetto; Tanira Alessandra Silveira Aguirre; Luiz Carlos Rodrigues Junior.
- **Writing – original draft** – Renata Zorzetto; Fernanda Poletto; Pedro Roosevelt Torres Romão; Tanira Alessandra Silveira Aguirre; Luiz Carlos Rodrigues Junior.
- **Writing – review & editing** – Renata Zorzetto; Tanira Alessandra Silveira Aguirre; Luiz Carlos Rodrigues Junior.

## 6. Acknowledgements

The authors are grateful to Coordenação de Aperfeiçoamento de Pessoal de Nível Superior (CAPES), Universidade Federal de Ciências da Saúde de Porto Alegre (UFCSPA), and Fundação de Amparo a Pesquisa no Rio Grande do Sul (FAPERGS).

## 7. References

1. Gupta, R., Warren, T., & Wald, A. (2007). Genital herpes. *Lancet*, 370(9605), 2127-2137. [http://doi.org/10.1016/S0140-6736\(07\)61908-4](http://doi.org/10.1016/S0140-6736(07)61908-4). PMID:18156035.
2. Looker, K. J., & Garnett, G. P. (2005). A systematic review of the epidemiology and interaction of herpes simplex virus types 1 and 2. *Sexually Transmitted Infections*, 81(2), 103-107. <http://doi.org/10.1136/sti.2004.012039>. PMID:15800084.
3. Looker, K. J., Magaret, A. S., May, M. T., Turner, K. M. E., Vickerman, P., Gottlieb, S. L., & Newman, L. M. (2015). Global and regional estimates of prevalent and incident herpes simplex virus type 1 infections in 2012. *PLoS One*, 10(10), e0140765. <http://doi.org/10.1371/journal.pone.0140765>. PMID:26510007.
4. Perng, G. C., & Jones, C. (2010). Towards an understanding of the herpes simplex virus type 1 latency-reactivation cycle. *Interdisciplinary Perspectives on Infectious Diseases*, 2010, 262415. <http://doi.org/10.1155/2010/262415>. PMID:20169002.
5. Garner, J. A. (2003). Herpes simplex virion entry into and intracellular transport within mammalian cells. *Advanced Drug Delivery Reviews*, 55(11), 1497-1513. <http://doi.org/10.1016/j.addr.2003.07.006>. PMID:14597143.
6. Frank, G. M., Lepisto, A. J., Freeman, M. L., Sheridan, B. S., Cherpès, T. L., & Hendricks, R. L. (2010). Early CD4 + T cell help prevents partial CD8 + T cell exhaustion and promotes maintenance of herpes simplex virus 1 latency. *Journal of Immunology*, 184(1), 277-286. <http://doi.org/10.4049/jimmunol.0902373>. PMID:19949087.
7. St. Leger, A. J., Peters, B., Sidney, J., Sette, A., & Hendricks, R. L. (2011). Defining the herpes simplex virus-specific CD8 + T cell repertoire in C57BL/6 mice. *Journal of Immunology*, 186(7), 3927-3933. <http://doi.org/10.4049/jimmunol.1003735>. PMID:21357536.
8. Treat, B. R., Bidula, S. M., Ramachandran, S., St Leger, A. J., Hendricks, R. L., & Kinchington, P. R. (2017). Influence of an immunodominant herpes simplex virus type 1 CD8+ T cell epitope on the target hierarchy and function of subdominant CD8+ T cells. *PLoS Pathogens*, 13(12), e1006732. <http://doi.org/10.1371/journal.ppat.1006732>. PMID:29206240.
9. Treat, B. R., Bidula, S. M., St. Leger, A. J., Hendricks, R. L., & Kinchington, P. R. (2020). Herpes simplex virus 1-specific CD8+ T cell priming and latent ganglionic retention are shaped by viral epitope promoter kinetics. *Journal of Virology*, 94(5), e01193-19. <http://doi.org/10.1128/JVI.01193-19>. PMID:31826989.
10. Koelle, D. M., Dong, L., Jing, L., Laing, K. J., Zhu, J., Jin, L., Selke, S., Wald, A., Varon, D., Huang, M.-L., Johnston, C., Corey, L., & Posavad, C. (2022). HSV-2-specific human female reproductive tract tissue resident memory t cells recognize diverse HSV antigens. *Frontiers in Immunology*, 13, 867962. <http://doi.org/10.3389/fimmu.2022.867962>. PMID:35432373.
11. Reardon, J. E., & Spector, T. (1989). Herpes simplex virus type 1 DNA polymerase: mechanism of inhibition by acyclovir triphosphate. *The Journal of Biological Chemistry*, 264(13), 7405-7411. [http://doi.org/10.1016/S0021-9258\(18\)83248-3](http://doi.org/10.1016/S0021-9258(18)83248-3). PMID:2540193.
12. Kost, R. G., Hill, E. L., Tigges, M., & Straus, S. E. (1993). Recurrent acyclovir-resistant genital herpes in an immunocompetent patient. *The New England Journal of Medicine*, 329(24), 1777-1782. <http://doi.org/10.1056/NEJM199312093292405>. PMID:8232486.
13. Kimberlin, D. W., Crumacker, C. S., Straus, S. E., Biron, K. K., Drew, W. L., Hayden, F. G., McKinlay, M., Richman, D. D., & Whitley, R. J. (1995). Antiviral resistance in clinical practice. *Antiviral Research*, 26(4), 423-438. [http://doi.org/10.1016/0166-3542\(95\)00031-G](http://doi.org/10.1016/0166-3542(95)00031-G). PMID:7574544.
14. Hanke, T., Graham, F. L., Rosenthal, K. L., & Johnson, D. C. (1991). Identification of an immunodominant cytotoxic T-lymphocyte recognition site gB of herpes simplex virus by using recombinant adenovirus vectors. *Journal of Virology*, 65(3), 1177-1186. <http://doi.org/10.1128/jvi.65.3.1177-1186.1991>. PMID:1847447.
15. Çuburu, N., Kim, R., Guittard, G. C., Thompson, C. D., Day, P. M., Hamm, D. E., Pang, Y.-Y. S., Graham, B. S., Lowy, D. R., & Schiller, J. T. (2019). A prime-pull-amplify vaccination strategy to maximize induction of circulating and genital-resident intraepithelial CD8 + memory T cells. *Journal of Immunology*, 202(4), 1250-1264. <http://doi.org/10.4049/jimmunol.1800219>. PMID:30635393.
16. Schaffazick, S. R., Guterres, S. S., Freitas, L. L., & Pohlmann, A. R. (2003). Caracterização e estabilidade físico-química de sistemas poliméricos nanoparticulados para administração de fármacos. *Química Nova*, 26(5), 726-737. <http://doi.org/10.1590/S0100-40422003000500017>.
17. Kumari, A., Yadav, S. K., & Yadav, S. C. (2010). Biodegradable polymeric nanoparticles based drug delivery systems. *Colloids and Surfaces. B, Biointerfaces*, 75(1), 1-18. <http://doi.org/10.1016/j.colsurfb.2009.09.001>. PMID:19782542.
18. Woodruff, M. A., & Hutmacher, D. W. (2010). The return of a forgotten polymer: polycaprolactone in the 21st century. *Progress in Polymer Science*, 35(10), 1217-1256. <http://doi.org/10.1016/j.progpolymsci.2010.04.002>.
19. Limayem Blouza, I., Charcosset, C., Sfar, S., & Fessi, H. (2006). Preparation and characterization of spironolactone-loaded nanocapsules for paediatric use. *International Journal of Pharmaceutics*, 325(1-2), 124-131. <http://doi.org/10.1016/j.ijpharm.2006.06.022>. PMID:16872764.
20. Fiel, L. A., Contri, R. V., Bica, J. F., Figueiró, F., Battastini, A. M. O., Guterres, S. S., & Pohlmann, A. R. (2014). Labeling the oily core of nanocapsules and lipid-core nanocapsules with a triglyceride conjugated to a fluorescent dye as a strategy to particle tracking in biological studies. *Nanoscale Research Letters*, 9(1), 233. <http://doi.org/10.1186/1556-276X-9-233>. PMID:24936156.



21. Oliveira, J. V. R., Silveira, P. L., Spingolon, G., Alves, G. A. L., Peña, F. P., & Aguirre, T. A. S. (2023). Polymeric nanoparticles containing babassu oil: a proposed drug delivery system for controlled release of hydrophilic compounds. *Chemistry and Physics of Lipids*, 253, 105304. <http://doi.org/10.1016/j.chemphyslip.2023.105304>. PMID:37080377.
22. Reis, M. Y. F. A., Santos, S. M., Silva, D. R., Silva, M. V., Correia, M. T. S., Ferraz Navarro, D. M. A., Santos, G. K. N., Hallwass, F., Bianchi, O., Silva, A. G., Melo, J. V., Mattos, A. B., Ximenes, R. M., Machado, G., & Saraiva, K. L. A. (2017). Anti-inflammatory activity of babassu oil and development of a microemulsion system for topical delivery. *Evidence-Based Complementary and Alternative Medicine*, 2017(1), 3647801. <http://doi.org/10.1155/2017/3647801>. PMID:29430254.
23. Intahphuak, S., Khonsung, P., & Panthong, A. (2010). Anti-inflammatory, analgesic, and antipyretic activities of virgin coconut oil. *Pharmaceutical Biology*, 48(2), 151-157. <http://doi.org/10.3109/13880200903062614>. PMID:20645831.
24. Campos, J. L. A., Silva, T. L. L., Albuquerque, U. P., Peroni, N., & Araújo, E. L. (2015). Knowledge, use, and management of the Babassu Palm (*Attalea speciosa* Mart. ex Spreng) in the Araripe Region (Northeastern Brazil). *Economic Botany*, 69(3), 240-250. <http://doi.org/10.1007/s12231-015-9315-x>.
25. Santos, L., & Loschi, M. (2019). Quebradeiras de coco babaçu preservam tradição no interior do Maranhão. *Revista Retratos*, 15, 1-28. Retrieved in 2024, April 21, from <https://agenciadenoticias.ibge.gov.br/agencia-noticias/2012-agencia-de-noticias/noticias/23624-quebradeiras-de-coco-babacu-preservam-tradicao-no-interior-do-maranhao>
26. Rodrigues, E. C. R., Ferreira, A. M., Vilhena, J. C. E., Almeida, F. B., Cruz, R. A. S., Amado, J. R. R., Florentino, A. C., Carvalho, J. C. T., & Fernandes, C. P. (2014). Development of babassu oil based nanoemulsions. *Latin American Journal of Pharmacy*, 34(2), 338-343. Retrieved in 2024, April 21, from [http://www.latamjpharm.org/resumenes/34/2/LAJOP\\_34\\_2\\_1\\_20.pdf](http://www.latamjpharm.org/resumenes/34/2/LAJOP_34_2_1_20.pdf)
27. Plaza-Oliver, M., Santander-Ortega, M. J., & Lozano, M. V. (2021). Current approaches in lipid-based nanocarriers for oral drug delivery. *Drug Delivery and Translational Research*, 11(2), 471-497. <http://doi.org/10.1007/s13346-021-00908-7>. PMID:33528830.
28. Leyva-Gómez, G., Piñón-Segundo, E., Mendoza-Muñoz, N., Zambrano-Zaragoza, M. L., Mendoza-Elvira, S., & Quintanar-Guerrero, D. (2018). Approaches in polymeric nanoparticles for vaginal drug delivery: A review of the state of the art. *International Journal of Molecular Sciences*, 19(6), 1549. <http://doi.org/10.3390/ijms19061549>. PMID:29882846.
29. Poletto, F. S., Fiel, L. A., Lopes, M. V., Schaab, G., Gomes, A., Guterres, S. S., Rossi-Bergmann, B., & Pohlmann, A. R. (2012). Fluorescent-labeled poly( $\epsilon$ -caprolactone) lipid-core nanocapsules: synthesis, physicochemical properties and macrophage uptake. *Journal of Colloid Science and Biotechnology*, 1(1), 89-98. <http://doi.org/10.1166/jcsb.2012.1015>.
30. Hilario, G. M., Sulczewski, F. B., Liszbinski, R., Mello, L. D., Hagen, G., Fazolo, T., Neto, J., Dallegrave, E., Romão, P., Aguirre, T., & Rodrigues, L. C., Jr. (2021). Development and immunobiological evaluation of nanoparticles containing an immunodominant epitope of herpes simplex virus. *IET Nanobiotechnology/IET*, 15(6), 532-544. <http://doi.org/10.1049/nbt2.12043>. PMID:34694744.
31. International Council on Harmonisation of Technical Requirements for Registration of Pharmaceuticals for Human Use. (2005). *ICH harmonised tripartite guideline: validation of analytical procedures: text and methodology Q2(R1)*. Geneva: ICH.
32. Brasil. Ministério da Saúde. Agência Nacional de Vigilância Sanitária. Diretoria Colegiada. (2017, 25 de julho). *Resolução RDC nº 166, de 24 de julho de 2017. Dispõe sobre a validação de métodos analíticos e dá outras providências*. Diário Oficial da República Federativa do Brasil, Brasília.
33. Justus, B., Kanunfre, C. C., Budel, J. M., Faria, M. F., Raman, V., Paula, J. P., & Farago, P. V. (2019). New insights into the mechanisms of French lavender essential oil on non-small-cell lung cancer cell growth. *Industrial Crops and Products*, 136, 28-36. <http://doi.org/10.1016/j.indcrop.2019.04.051>.
34. Lopes, C. E., Langoski, G., Klein, T., Ferrari, P. C., & Farago, P. V. (2017). A simple hplc method for the determination of halcinonide in lipid nanoparticles: development, validation, encapsulation efficiency, and in vitro drug permeation. *Brazilian Journal of Pharmaceutical Sciences*, 53(2), e15250. <http://doi.org/10.1590/s2175-97902017000215250>.
35. Sutariya, V., Wehrung, D., & Geldenhuys, W. J. (2012). Development and validation of a novel RP-HPLC method for the analysis of reduced glutathione. *Journal of Chromatographic Science*, 50(3), 271-276. <http://doi.org/10.1093/chromsci/bmr055>. PMID:22337804.
36. Chaudhari, S. P., & Dugar, R. P. (2017). Application of surfactants in solid dispersion technology for improving solubility of poorly water soluble drugs. *Journal of Drug Delivery Science and Technology*, 41, 68-77. <http://doi.org/10.1016/j.jddst.2017.06.010>.
37. Patel, A., Patel, M., Yang, X., & Mitra, A. (2014). Recent advances in protein and peptide drug delivery: a special emphasis on polymeric nanoparticles. *Protein and Peptide Letters*, 21(11), 1102-1120. <http://doi.org/10.2174/0929866521666140807114240>. PMID:25106908.
38. Kim, M. R., Feng, T., Zhang, Q., Chan, H. Y. E., & Chau, Y. (2019). Co-encapsulation and co-delivery of peptide drugs via polymeric nanoparticles. *Polymers*, 11(2), 288. <http://doi.org/10.3390/polym11020288>. PMID:30960272.
39. McClements, D. J. (2018). Encapsulation, protection, and delivery of bioactive proteins and peptides using nanoparticle and microparticle systems: a review. *Advances in Colloid and Interface Science*, 253, 1-22. <http://doi.org/10.1016/j.cis.2018.02.002>. PMID:29478671.
40. Falciani, C., Zevolini, F., Brunetti, J., Riolo, G., Gracia, R., Marradi, M., Loinaz, I., Ziemann, C., Cossio, U., Llop, J., Bracci, L., & Pini, A. (2020). Antimicrobial peptide-loaded nanoparticles as inhalation therapy for *Pseudomonas aeruginosa* infections. *International Journal of Nanomedicine*, 15, 1117-1128. <http://doi.org/10.2147/IJN.S218966>. PMID:32110011.
41. Casciaro, B., d'Angelo, I., Zhang, X., Loffredo, M. R., Conte, G., Cappiello, F., Quaglia, F., Di, Y.-P. P., Ungaro, F., & Mangoni, M. L. (2019). Poly(lactide-co-glycolide) nanoparticles for prolonged therapeutic efficacy of esculetin-1a-derived antimicrobial peptides against *Pseudomonas aeruginosa* lung infection: in vitro and in vivo studies. *Biomacromolecules*, 20(5), 1876-1888. <http://doi.org/10.1021/acs.biomac.8b01829>. PMID:31013061.
42. Frank, L. A., Contri, R. V., Beck, R. C. R., Pohlmann, A. R., & Guterres, S. S. (2015). Improving drug biological effects by encapsulation into polymeric nanocapsules. *Wiley Interdisciplinary Reviews. Nanomedicine and Nanobiotechnology*, 7(5), 623-639. <http://doi.org/10.1002/wnan.1334>. PMID:25641603.
43. Frank, L. A., Sandri, G., D'Autilia, F., Contri, R. V., Bonferoni, M. C., Caramella, C., Frank, A. G., Pohlmann, A. R., & Guterres, S. S. (2014). Chitosan gel containing polymeric nanocapsules: a new formulation for vaginal drug delivery. *International Journal of Nanomedicine*, 9(1), 3151-3161. <http://doi.org/10.2147/IJN.S62599>. PMID:25061292.
44. Frank, L. A., Chaves, P. S., D'Amore, C. M., Contri, R. V., Frank, A. G., Beck, R. C. R., Pohlmann, A. R., Buffon, A., & Guterres, S. S. (2017). The use of chitosan as cationic coating or gel vehicle for polymeric nanocapsules: increasing penetration

- and adhesion of imiquimod in vaginal tissue. *European Journal of Pharmaceutics and Biopharmaceutics*, 114, 202-212. <http://doi.org/10.1016/j.ejpb.2017.01.021>. PMID:28161547.
45. Harshyne, L. A., Watkins, S. C., Gambotto, A., & Barratt-Boyes, S. M. (2001). Dendritic cells acquire antigens from live cells for cross-presentation to CTL. *Journal of Immunology*, 166(6), 3717-3723. <http://doi.org/10.4049/jimmunol.166.6.3717>. PMID:11238612.
46. Nayak, J. V., Hokey, D. A., Larregina, A., He, Y., Salter, R. D., Watkins, S. C., & Falo, L. D., Jr. (2006). Phagocytosis induces lysosome remodeling and regulated presentation of particulate antigens by activated dendritic cells. *Journal of Immunology*, 177(12), 8493-8503. <http://doi.org/10.4049/jimmunol.177.12.8493>. PMID:17142747.
47. Kong, B., Seog, J. H., Graham, L. M., & Lee, S. B. (2011). Experimental considerations on the cytotoxicity of nanoparticles. *Nanomedicine*, 6(5), 929-941. <http://doi.org/10.2217/nmm.11.77>. PMID:21793681.

Received: Apr. 21, 2024

Revised: Oct. 08, 2024

Accepted: Dec. 18, 2024